Contents lists available at http://qu.edu.iq

Al-Qadisiyah Journal for Engineering Sciences

Journal homepage: http://qu.edu.iq/journaleng/index.php/JQES

Effects of roof angle, inlet gap size and drying time on dryer mass flow rate and moisture content in a chimney-dependent solar crop dryer using design of experiments (DOE)

Anthony Agyei-Agyemang[a]*, Peter Oppong Tawiah[a], John K. Afriyie[b] and Michael K. Commeh[c]

[a]*Department of Mechanical Engineering, College of Engineering, Kwame Nkrumah University of Science and Technology, Kumasi, Kumasi, Ghana.*
[b]*Department of Mechanical Engineering, Kumasi Technical University, Kumasi, +233, Ghana.*
[c]*Technology Consultancy Centre, College of Engineering, Kwame Nkrumah University of Science and Technology, Kumasi, +233, Ghana.*

ARTICLE INFO

Article history:
Received 09 October 2021
Received in revised form 6 December 2021
Accepted 15 January 2022

Keywords:
Solar dryer
Roof angle
Inlet gap size
Multilevel factorial design
Moisture content
Ghana

ABSTRACT

A chimney dependent solar crop dryer (CDSCD) was designed and developed. Design of Experiments (DOE) was used to carry out experiments using a statistical three level non randomized factorial experimental design in Minitab statistical software version 19.0. The effect of three drying parameters, roof angle (º), Inlet gap size (mm), and time (h) on dryer inlet mass flow rate (kg/s) and moisture content (%) were studied. The regression results showed that there was a satisfactory fit of the model variability for both dryer inlet mass flow rate and crop moisture content. The p-value for each parameter was less than 0.005, which is statistically significant. The R-squared (R^2) value was 94.67% for inlet air mass flow rate study and 99.72% for moisture content. It was observed that the optimal values for achieving a low moisture content response (≤ 24%) were roof angle of 81º, inlet to outlet cross-sectional area ratio of 1.08768:1 and a minimum drying time of 24 hours while the optimal values for achieving high inlet air mass flow rate (≥ 0.357 kg/s) were roof angle of 51º, inlet to outlet cross-sectional area ratio of 1.08768:1 and a minimum drying time of 5 hours. The findings could be implemented and utilized for achieving optimum ventilation and drying performances to refine dryer (CDSCD) design.

1. Introduction

MOFA [1] observed that although agriculture is the largest sector of the economy in Ghana, contributing about 39% of GDP, it is still confronted with high post-harvest losses as a result of poor post-harvest management. For instance, Zakari [2] estimates that the average postharvest loss of mango is between 20 % and 50 %. The main causes for the losses being attributed to fruit flies, diseases, poor management, and storage during transit to the market. Drying, if used effectively, could minimize crop losses. Crop drying refers to the process of removing moisture from a crop. Solar dryer is a solar energy application in drying and conserving agricultural food products and other products [3]. Traditionally, farmers spread their crops on mats in the open sun to dry them, therefore exposing them to environmental conditions such as rain, pests, rodents and different types of unhygienic conditions. Harnessing solar energy is becoming more and more popular in drying. In solar drying, solar energy is the main source of energy used. Recent studies have shown that using solar energy in preserving agricultural products like grains, fruits, and vegetables is economical and ideal for farmers in the developing countries [4]. However,

* *Corresponding author.*
E-mail address: tonyagyemang@yahoo.com (Anthony Agyei-Agyemang)

https://doi.org/10.30772/qjes.v15i1.802

the use of solar energy alone as the source of heat for drying and preservation during the rainy season, is not feasible and therefore proves difficult [5]. As a result, it calls for different ways in which the solar energy is utilized to overcome the challenge. Different designs for drying have been proposed and tested to solve these problems.

The use of a chimney allows improved ventilation. A dryer's chimney combined with an inclined roof, inclined at right angle in a drying chamber design, when coupled with a suitable inlet exit area ratio, was observed to increase the ventilation in direct mode dryer [6-10]. A solar dyer with a tent dryer architecture, generally works on the principle that in operation, radiant energy of short wavelength from the sun is transmitted through transparent drying chamber and chimney glazing to fall on absorbers in the dryer. The absorbers, after absorbing this radiant energy, in turn emit heat energy of long wavelength that gets trapped but does not pass through the glazing back into the atmosphere. The trapped energy heats up the air in the chamber and chimney and effectively dries the product in the drying chamber. That is, cold air flows through the dryer by entering the bottom inlet, gets heated up and dries the crops inside the drying chamber. During this process, the air absorbs moisture from the crops and flows through the solar chimney where its density drops after absorbing more heat and is then driven upwards to exit through the top vent into the surroundings, effecting a continuous flow where the cold, dense air is drawn in to displace the warm air flowing through the dryer [6-10]. It has been confirmed by other researchers that properly designed solar chimneys have been observed to improve the flow of air in an enclosed chamber [11-15].

Generally, high amount of moisture in dried seeds increases incidence of insect infestation and growth of microorganisms. Fast drying of agro-products reduces their moisture content and therefore prevents conditions favorable for the growth of fungi and microorganisms that affect food quality during storage [16]. Molds that produce aflatoxins (Aspergillus flavus) also grow on products stored under conditions with high relative humidity and temperature [18-19]. Aflatoxins can cause many different health issues and diseases like liver cancer, renal diseases, and gastroenteritis, and they could also be associated with child growth impairment [20]. The rate of insect infestation of post-harvest crops worsens with increase in relative humidity and temperature.

Drying could be classified generally into three: Sun, Mechanical, and Solar drying. Sun drying is the direct exposure of a product to the sun on a surface, resulting in direct heating by solar radiation and eventual removal of moisture through circulation of air, naturally. Sun drying needs no additional source of energy other than sunlight and is therefore the cheapest method of drying [21]. However, this method is not efficient and is also labor and time intensive. It is not efficient because natural air flowing around the crop to be dried could introduce moisture and also remove essential heat which otherwise could enhance the drying process [22]. Mechanical drying is a process in which heat is introduced artificially to increase the drying medium's temperature to cause evaporation of excess moisture from a product. The heat source is usually either fossil fuel or electricity. Major types of mechanical dryers include bin, cabinet, mixed flow, and continuous cross flow dryers. The solar dryer is the third group and the most economically sustainable option for developing countries. A solar dryer, unlike sun drying, is a customized enclosure which regulates the process of drying and shields the product against contamination with dust and rain, as well as infestation with insects [23], thereby reducing the drying time significantly, and improving the quality of dried product vis a vis that of sun drying [24]. That is, the drying temperature rises as the relative humidity falls, resulting in a reduced moisture content in dried product. Solar dryers come in different forms. They may be classified as direct or indirect, based on whether the material to be dried is exposed to direct insolation or not. On the other hand, they may be classified based on the mechanism of air flow through the dryer, thus solar dryers can be either natural convection solar dryers or forced convection solar dryers [17]. Air flows through such dryers due to thermally induced density gradient. In dryers using forced convection, a pressure difference, generated by a fan, forces air to flow through the drying chamber [17].

On the other hand, based on indirect or direct solar dryer classification, in the indirect solar dryer, a solar collector is used to heat the air entering the drying chamber. Through convection heat is exchanged between the crop being dried and the hot air, and in the process heated air is forced to flow on the drying bed to remove moisture [21]. Though there are different drying methods for food products, drying food in an indirect solar dryer is a prominent technology nowadays [25]. The direct solar dryer, is one in which a frame covered with transparent material and the sides protected with boards is used to protect the product being dried. The product to be dried and the drying chamber's inner surfaces absorb solar radiation, and thus raise the product temperature and that of its enclosure to effect drying [26]. The direct dryers are appropriate for locations that have direct sunshine for long periods during day time [4]. Mixed mode solar dryers integrate characteristics of both direct and indirect solar dryers [21]. Heat needed to dry the produce is partly supplied by the solar collector which pre-heats the air and by direct solar insolation on the produce [26]. Lingayat et al. [27] reports that the indirect mode dryer could be more effective and efficient than the direct mode dryer. Another category of solar drying is the Hybrid solar dryer. Hybrid solar dryers go a step further to make the dryer operational even during cloudy periods. In addition to using solar energy, hybrid systems incorporate other means of heating the air for drying a produce.

All solar dryers have a means to let out exhaust air. Most solar dryers let out exhaust air which collected moisture from the produce to be dried through a chimney. The air passes through the drying chamber and then flows out through the chimney due to the buoyancy effect or stack effect [28]. Nasution et. al. [29] and Abedini et al. [30], studied deep bed drying performance on paddy and shrimp respectively, using hybrid infrared-solar dryer and found it to be more effective than solar dryer only. Using an organic paraffin wax, with a melting point of 60 ℃ as phase change material (PCM) in a solar dryer chamber with black stones as the base, Radhakrishnan et al., [31] dried coconut from an initial moisture content of 55.5% to a final moisture content of about 9%, observing that the drying time of coconut decreased by about 28 and 52 h on using 100 g and 200 g of PCM, respectively, compared to open sun drying; the sensory characteristics like color, taste, flavors, quality, and texture of the dried coconut sample were superior to the sun-dried coconut sample. Senthil et al., [32] also found the integration of PMC in the solar dryer to enhance drying and reduced drying time up to 60% over a solar dryer without PCM. Afriyie [6] observed from trials on a CDSCD that even though open sun drying could proceed very well at the initial phases of drying, the CDSCD always finishes the drying process faster. Therefore, improving on direct solar dryer is good and worth exploring. Afriyie [6] cautioned that, relying on one particular feature of the CDSCD for performance improvement may render the dryer uneconomical or unstable, and recommended that a reasonable moderate change in two or more features, or design characteristics, could be the best method of improvement of a CDSCD. Design of experiments (DOE) is a good method of studying the combined effects of two or more features on a system and was therefore used for this study. Design of Experiments (DoE) is a statistical method that allows the variation of different factors and combination of factors at the same time to study a system for optimum values [33].

Design of Experiment (DOE) has so many advantages over traditional experimental methods where most of the time one parameter is studied at a time and then through try-and-error modifications are made in new experiments to improve a system. Some of the advantages of DOE include the ease of its use in the evaluation, comparison and optimization of design configurations, evaluation of possible material alternatives, selection of design parameters and configurations for robust products that can work under different field and environmental conditions [34]. Ultimately, DOE

allows one to make more informed decisions during the problem-solving process, and conclude with better solutions within a shorter time [33]. The main disadvantages of DOE are that it requires a lot of skills, strong knowledge of statistical methods, discipline and effective communication between members of a project team for it to work reliably [33]. It can therefore be concluded that DOE improves process yields, reduces variability, promote closer conformance to nominal or target requirements and specifications, reduces development time, and reduces overall costs [34]. Therefore, DOE was selected as the method for this study.

2. Materials and methods

2.1. Experimental works

A laboratory scale model for the CDSCD with three (3) substitutable roofs (each with diverse roof angles oriented to the vertical plane) was fabricated. The roof angles were oriented at 51°, 64° and 81°.

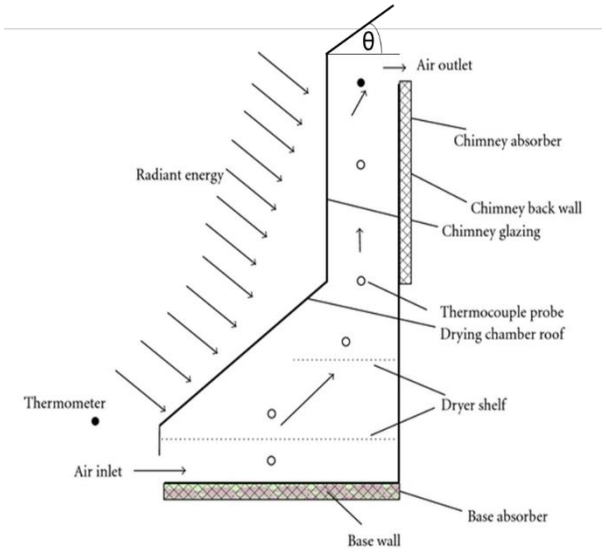

Figure 1. Functional architecture of CDSCD.

Lexan sheet was used as glazing material for the drying chamber walls. The drying chamber width positioned normal to air flow was 440 mm and the length in air flow direction was 530 mm. 40 mm thick wood was used as the base of the dryer with the topmost surface of the wood painted black to function as a heat absorber of the dryer. Three plates of Lexan sheet with a length covering the dryer's width were placed at the inlet to set inlet gaps at 30, 50 and 70 mm during the experiment. A steel grate with a width of 400 mm and a length of 370 mm was placed 150 mm above the base of the dryer to serve as a drying shelf. Two extra meshes, each with about half the length of the first mesh, were also used for different shelf configurations during the drying process. The chimney had a rectangular cross-section (400 mm width, uniform gap of 80 mm and a height of 625 mm). The dryer exit was oriented at right angles to the chimney cross-section at the top and had an exit gap which was 30 mm, and a width of 335 mm but curved at the ends at a radius of 15 mm. Lexan sheet glazing material was used as the walls of the chimney.

A removable back wall of wood constructions with an internal black painted surface was used as chimney absorber. Solar irradiation was simulated by setting up eight 100 W infrared lamps in front of the dryer. Thermocouple probes, handheld anemometer and handheld thermo-hygrometer were used to record temperature, relative humidity and air velocities within and outside the drying chamber. Details of instrumentation setup can be found in Afriyie [6] and Afriyie et al. [7]. Figures 1 and 2 present a sketch of the functional architecture and pictorial view of the laboratory setup for the CDSCD. of the dryer tray arrangements and the pictorial view of the field setup respectively.

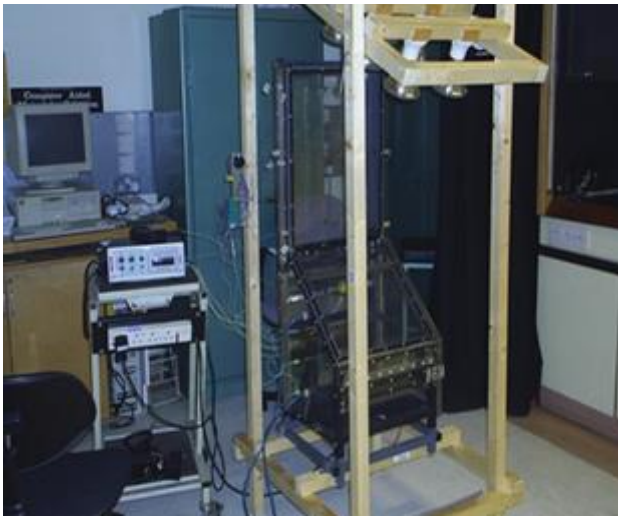

Figure 2. Picture of the laboratory setup of CDSCD.

2.2. Design of Experiments

Design of Experiments (DOE) was used. The designed drying experiments were carried out using statistical three level non randomized factorial experimental design which was implemented in Minitab statistical software version 19.0. Five drying parameters were considered in this experiment namely: Roof angle (º), Inlet gap size (mm), drying time (cm), dryer inlet mass flow rate (kg/s) and moisture content (%). The dryer inlet mass flow rate effects had a total of 216 runs, and the moisture content effects had 225 runs. Presented in Table 1 is the design summary for the inlet mass flow rate, and moisture content effects experiments. Table 2 gives the experimental design summary for the effects of roof angle, inlet gap size and time on both inlet mass flow rate, and moisture content. From Table 2, the experiments consist of three factors: roof angle and inlet gap size with three levels each, and time with 24 levels.

Table 1. Design summary for the inlet mass flow rate and moisture content effects experiments.

Design Summary							
Inlet mass flow rate effects study				Moisture content effects study			
Factors:	3	Replicates:	1	Factors:	3	Replicates:	1
Base runs:	216	Total runs:	216	Base runs:	225	Total runs:	225
Base blocks:	1	Total blocks:	1	Base blocks:	1	Total blocks:	1

Table 2. The experimental matrix for effects of roof angle, inlet gap size and time on inlet mass flow rate, and moisture content.

Factor	Level Values						
	1st	2nd	3rd	4th	5th	6th	7th … 23rd
Roof Angle (°)	51	64	81	-	-	-	-
Inlet Gap, (mm)	30	50	70	-	-	-	-
Time (h)	1, 2, 3, 4, 5, 6, 7, 8,9,10,11, 12, 13, 14, 15, 16, 17, 18, 19, 20, 21, 22, 23, 24						

3. Results and discussions

The effects of roof angle, inlet gap size and time on dryer inlet mass flow rate is presented in section 3.1 while the effects of roof angle, inlet gap size and time on dryer moisture content is discussed in section 3.2.

3.1. Effects of roof angle, inlet gap size and time of dryer on inlet air mass flow rate

The Pareto chart of standardized effects for mass flow rate response with the confidence level set at 0.05 is shown in Figure 3. From Figure 3, time (A), inlet gap (B), roof angle (C), interaction of time and inlet gap (AB), interaction of time and roof angle (AC), and interaction of inlet gap and roof angle (BC) have 7.6, 7.4, 5.8, 3.3, 0.4 and 0.6 standardized effect values respectively. The Pareto chart shows that time has the highest standardized effect (7.6) on the dryer inlet mass flow rate while AC (time and roof angle) has the least standardized effect of 0.4. Aside from the individual factors (A, B and C), interaction of time and inlet gap (AB) also has a significant effect on the dryer inlet air mass flow rate.

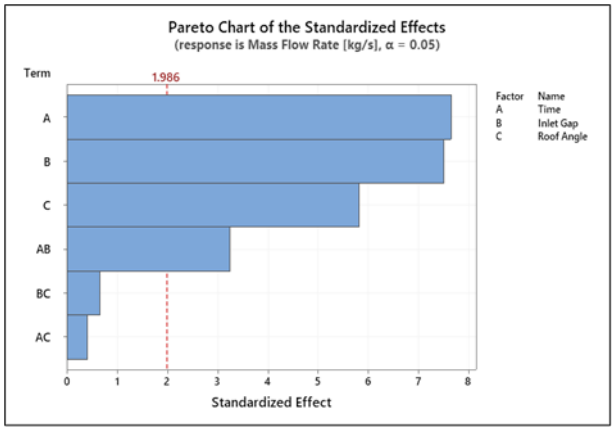

Figure 3. Pareto chart of standardized effects (Inlet mass flow rate response).

The p-values, which are good metrics to evaluate a statistical model, were calculated and presented together with the F-values, degrees of freedom and the mean-squares in Table 3. The p-value for each term (roof angle, inlet gap, and time) was less than 0.005 which is statistically significant. Figure 4 presents residual plots for inlet mass flow rate. From the residual plots, the pattern for normal probability plot is an S-curve which indicates a distribution with long tails. The residuals versus fits plot confirms the assumption that the residuals are randomly distributed and have a nonconstant variance with uneven spreading of residuals across fitted values as points are random on both sides of the zero-line (0) with no patterns in the point positions. Histogram plot pattern depicts long tails in both (right and left) directions which indicates a general skewness in the model. Some few bars lie far away on the left and right sides which indicates an outlier pattern. The residuals in residuals versus order plot appear randomly, close to the centre line, giving a pattern that shows independent residuals. The residual plots for air inlet mass flow rate show that the result is satisfactory.

Table 3. The analysis of variance results for effects of roof angle, inlet gap size and time on inlet mass flow rate.

Source	DF	Adj SS	Adj MS	F-Value	P-Value
Model	123	0.000648	0.000005	13.28	0.000
Linear	27	0.000593	0.000022	55.37	0.000
Roof Angle (deg)	23	0.000553	0.000024	60.57	0.000
Inlet Gap (mm)	2	0.000025	0.000012	31.44	0.000
Time (h)	2	0.000015	0.000008	19.46	0.000
2-Way Interactions	96	0.000055	0.000001	1.44	0.039
Roof Angle (deg)*Inlet Gap (mm)	46	0.000038	0.000001	2.06	0.002
Roof Angle (deg)*Time (h)	46	0.000016	0.000000	0.87	0.688
Inlet Gap (mm)*Time (h)	4	0.000001	0.000000	0.83	0.510
Error	92	0.000037	0.000000		
Total	215	0.000685			

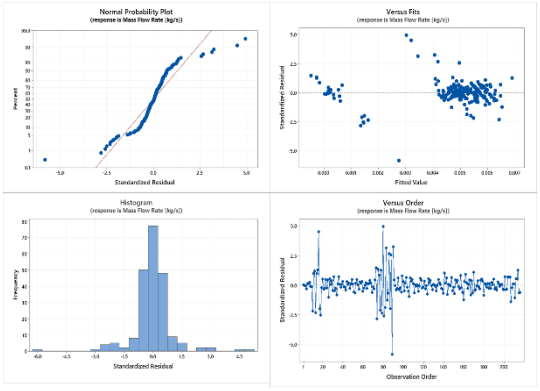

Figure 4. Residual plots for inlet mass flow rate.

Degrees of freedom (DF), sum of squares (SS), mean squares (MS)(Variance), ratio of variance of a source to variance of error (F), significance of a factor at 95% confidence level ($P < 0.05$). A summary of computed regression values is presented in Table 4. R-squared (R^2) which represents a goodness of fit measure for linear regressions was 94.67%. The adjusted values of R-squared (R-sq(adj)) and predicted values of R-Squared (R-sq(pred)) were 87.54% and 70.61% respectively. These regression results show a satisfactory fit of the model variability for the dryer inlet mass flow rate.

Table 4. The analysis of variance results for effects of roof angle, inlet gap size and time on inlet mass flow rate summary model

S	R-sq	R-sq(adj)	R-sq(pred)
0.0006300	94.67%	87.54%	70.61%

The main effect plot for inlet mass flow rate is shown in Figure 5. From Figure 5, a roof angle of 51º shows the highest mean mass flow rate at inlet to be 0.00495 kg/s; whilst the other roof angles show lower effects on mean inlet mass flow rate (roof angles of 64º and 81º yielded 0.00461 kg/s and 0.004296 kg/s respectfully). The inlet gap of 30 mm influenced a mean inlet mass flow rate effect of 0.00414 kg/s. The inlet gaps of 50 mm and 70 mm attained mean inlet mass flow rate of 0.00480961 kg/s and 0.0049035 kg/s respectively. Time of drying which plays a significant role in any drying process yielded higher mean mass flow rate at the inlet of 0.0.0053482 kg/s at 5 hours into the drying, 0.00541763 kg/s at 14 hours into the drying and 0.00553361 kg/s at the end of the drying process at 24 hours. The interaction plot for mass flow rate at inlet, showing the various mean inlet mass flow rates and the interaction between various drying factors (roof angle, inlet gap and drying time), is shown in Figure 6. The highest mean of inlet mass flow rate for the interaction between roof angle and inlet gap is 0.00534223 kg/s. From Figure 6, the roof angle and time interaction show the highest mean inlet mass flow 0.00593005 kg/s at 19 hours drying time. The following drying time periods (hours) for the 51 º roof angle attained high mean inlet mass flow rates above 0.00534223 kg/s: they are 15, 16, 17, 18, 19, 20, 21 22, 23 and 24 hours.

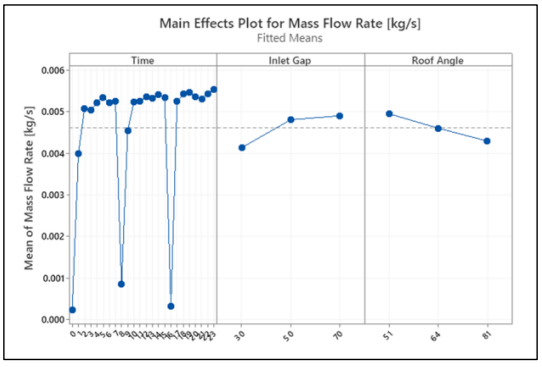

Figure 5. Main effects plot for inlet mass flow rate.

A response optimization was carried out to select the optimum factor values necessary to achieve high inlet mass flow rate to accelerate drying. Figure 7 presents the optimization plot after carrying out response optimization. The optimal values for achieving very high inlet mass flow rate response ($\geqslant$ 0.0069 kg/s) are roof angle of 51º, inlet gap of 30 mm and a minimum drying time of five hours.

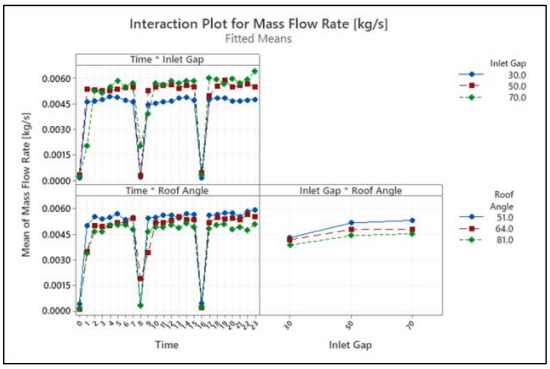

Figure 6. Interaction plot for inlet mass flow rate.

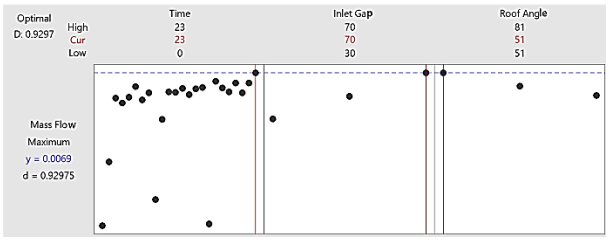

Figure 7. Optimization plot.

3.1. Effects of roof angle, inlet gap size and time on moisture content

Figure 8 presents the Pareto chart of standardized effects for moisture content response at a confidence level of 95%. Roof angle (A), interaction of roof angle and inlet gap (AB), inlet gap (B) and time (C) had the same standardized effect of 7.6. Roof angle and time interaction (AC), and Inlet gap and Time interaction (BC) had 0.6 and 0.1 standardized effects respectfully, which are below the reference line (1.985), and are therefore not significant.

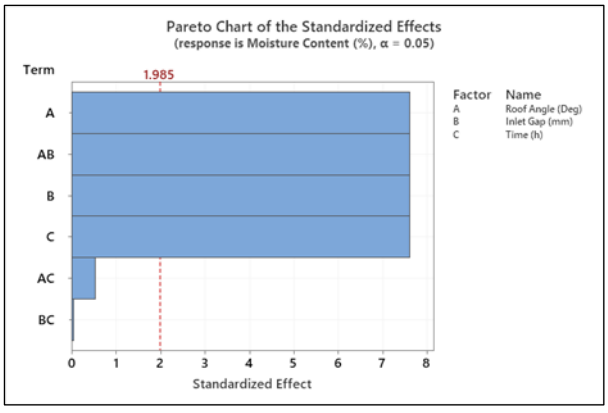

Figure 8. Pareto chart of standardized effects (moisture response)

Table 4 shows analysis of variance results for effects of roof angle, inlet gap size and time on moisture content. The p-value for each term (roof angle, inlet gap and time) was less than 0.005, which is statistically significant.

Table 5. The analysis of variance results for effects of roof angle, inlet gap size and time on inlet mass flow rate.

Source	DF	Adj SS	Adj MS	F-Value	P-Value
Model	128	582889	4553.8	270.23	0.000
Linear	28	576961	20605.8	1222.79	0.000
Roof Angle (deg)	2	3808	1903.8	112.97	0.000
Inlet Gap (mm)	2	2712	1355.9	80.46	0.000
Time (h)	24	570442	23768.4	1410.46	0.000
2-Way Interactions	100	5927	59.3	3.52	0.000
Roof Angle (deg)*Inlet Gap (mm)	4	4660	1165.1	69.14	0.000
Roof Angle (deg)*Time (h)	48	758	15.8	0.94	0.591
Inlet Gap (mm)* Time (h)	48	509	10.6	0.63	0.961
Error	96	1618	16.9		
Total	224	584506			

The models fitted the data well. A summary of computed regression values is presented in Table 5. The R-squared (R^2) which represents a goodness of fit measure for linear regressions was 99.72%. The derived adjusted R-squared values (R-sq(adj)) and predicted R-Squared values (R-sq(pred)) were 99.35% and 98.48% respectfully. These regression results show a satisfactory fit of the model variability for the crop moisture content.

Table 6. Regression model summary model

S	R-sq	R-sq(adj)	R-sq(pred)
4.10506	99.72%	99.35%	98.48%

Presented in Figure 9 are residual plots for moisture content. The pattern for normal probability plot shows a few points lying away from the line which implies a distribution with outliers. The residuals versus fits plot verifies the assumption that residuals are randomly distributed and have a nonconstant variance with fanning or uneven spreading of residuals across fitted values as the points randomly appear on both sides of the zero line (0) with no recognizable patterns in the points. The histogram plot pattern depicts long tails on both (right and left) directions which indicate a general skewness in the model. The residuals in the residuals versus order plot are distributed randomly around the centre line and the pattern formed indicate that the residuals are independent. In summary the residual plot results show a good model fit.

The main effects plot for moisture content is shown in Figure 10. The highest mean value of moisture content for roof angle effect was 119% at a roof angle of 51º. Roof angle of 64º and 81º recorded mean moisture content of 113.5% and 108% respectfully. For inlet gap effect, the lowest mean moisture content measured was 108% at inlet gap of 30 mm. The highest mean moisture content was 117% at inlet gap of 70 mm and the next was mean moisture content of 115% at 50 mm inlet gap. For effect of temperature, the highest mean moisture content drop was from 202 % to 24%, and it occurred after 24 hours. This shows the time dependency nature of a typical drying process

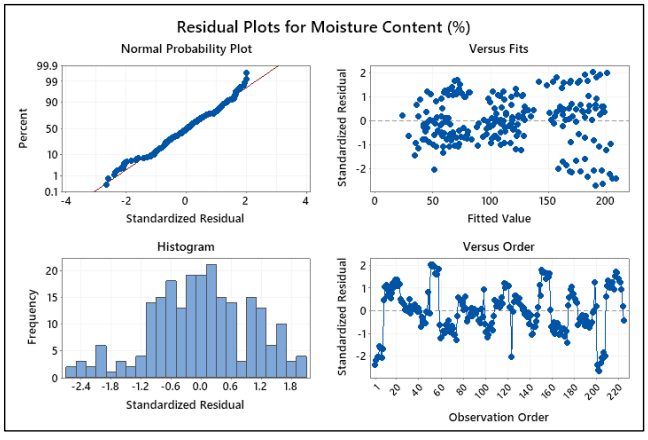

Figure 9. Residual plots for moisture content.

. Figure 11 presents interaction plot for moisture content. The lowest mean moisture content response recorded for interaction of roof angle and inlet gap was 90% at 81º and 30 mm; whilst the highest was 140% at 64º roof angle and 50 mm inlet gap. The next mean moisture content recorded was 135%, at 64º and 70 mm. Results from Figure 11 show that interaction between roof angle and time and interaction between inlet gap and time were heavily influenced by the time factor; the lowest recorded was after 24 hours for both as 24% at roof angle of 81º and inlet gap of 30 mm.

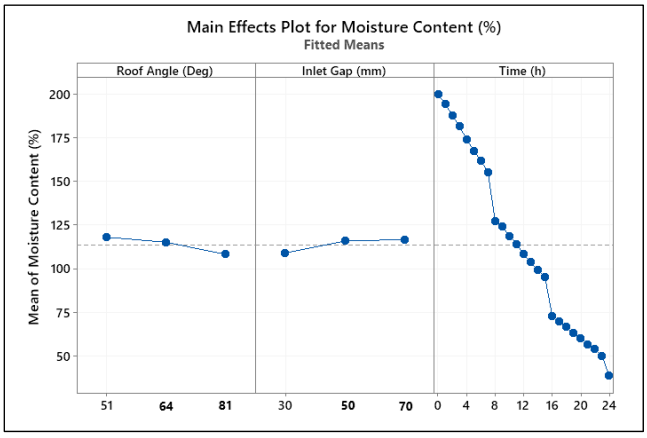

Figure 10. Main effects plot for moisture content.

The results of optimization response prediction presented in Figure 12 shows the optimal values which will improve drying efficiency. The optimal values for achieving low moisture content response (⩽ 24%) are roof angle of 81º, inlet gap of 30 mm and a minimum drying time of 24 hours. The 30 mm inlet gap implies an inlet area of 0.03 m × 0.39 m or 0.0117 m^2 inlet cross-sectional area. With exit cross-sectional area of 0.03 m × 0.335 m with two (2) semi circles with 15 mm radius on either side of the exit, giving a cross-sectional area of 0.0107568 m^2. Thus, the optimum inlet to outlet area ratio is 1.08768:1.

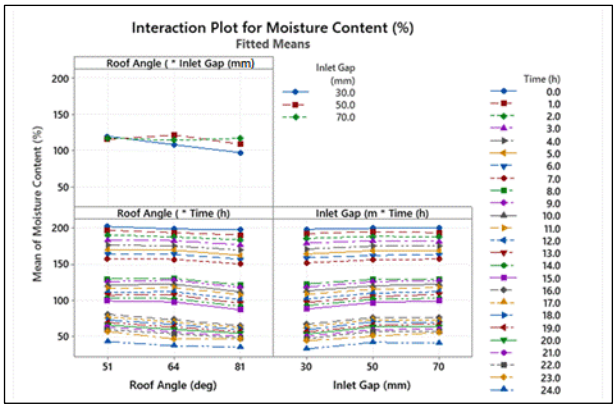

Figure 11. Interaction plot for moisture content.

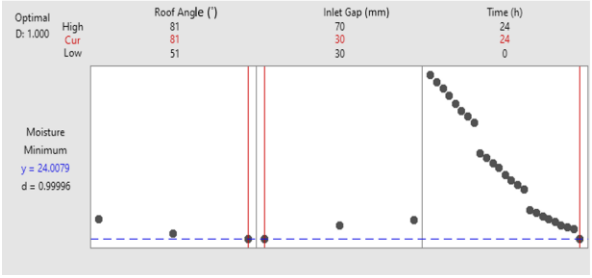

Figure 12. Optimization plot for moisture content.

4. Conclusions

From the study on effects of roof angle, inlet gap size and time on moisture content it can be concluded that the optimal values for achieving low moisture content response ($\leq 24\%$) are such that for a given ambient relative humidity, a roof angle of 81º, an inlet gap such that the inlet to outlet area ratio is 1.08768:1 and minimum drying time of 24 hours. On the other hand, from the study of effects of roof angle, inlet gap size and time on dryer inlet air mass flow rate, the optimal values for achieving high inlet air mass flow rate (≥ 0.0069 kg/s) are such that for a given ambient relative humidity, a roof angle of 51º, an inlet gap which gives inlet to outlet cross-sectional area ratio of 1.08768:1 and a minimum drying time of five hours. That is, for good drying conditions for a given ambient relative humidity is such that, an inlet gap which gives an inlet to outlet cross-sectional area ratio of 1.08768:1, drying time of at least 24 hours, and roof angle of either 51º or 81º are desirable. Since the ultimate focus of a dryer is to reduce moisture content of the product in the dryer, the 81º, which gives the minimum moisture content, should be preferred. The findings can be used as a guide and tool to compare various designs of dryers to improve ventilation and ultimately to target optimum design and improved drying performance of CDSCD dryers.

Authors' contribution

All authors contributed equally to the preparation of this article.

Declaration of competing interest

The authors declare no conflicts of interest.

Funding source

This study didn't receive any specific funds.

REFERENCES

[1] MoFA (2011). Statistics, Research and Information Directorate (SRID). Agriculture in Ghana.

[2] Zakari, A. K. (2012). Ghana National Mango Study. PACT II Program and International Trade Centre Ghana.

[3] Kumar, K. R., Chaitanya, N. K., and Kumar, N. S. (2021). Solar thermal energy technologies and its applications for process heating and power generation–A review. Journal of Cleaner Production, 282, 125296, https://doi.org/10.1016/j.jclepro.2020.125296

[4] Mustayen, A. G. M. B., Mekhilef, S., & Saidur, R. (2014). Performance study of different solar dryers: A review. *Renewable and Sustainable Energy Reviews*, *34*, 463–470. https://doi.org/10.1016/j.rser.2014.03.020

[5] Barki, E., Ibrahim, J.S. and Eloka-Eboka, A. C. (2012). Performance Evaluation of an Efficient Solar Dryer with a Backup Incinerator for Grated Cassava under Makurdi Humid Climate. *International Journal of Environment and Bioenergy*, *2*(2): 131–139.

[6] Afriyie J. K. (2007) Design, Simulation and Optimisation of a Chimney-Dependent Direct-Mode Solar Crop Dryer (CDSCD), PhD Thesis, De Montfort University, Leicester-England.

[7] Afriyie, J. K., Nazha, M. A. A., Rajakaruna, H., & Forson, F. K. (2009). Experimental investigations of a chimney-dependent solar crop dryer. *Renewable Energy*, *34*(1), 217–222. https://doi.org/10.1016/j.renene.2008.04.010

[8] Afriyie, J. K., Rajakaruna, H., Nazha, M. A. A., & Forson, F. K. (2011). Simulation and optimisation of the ventilation in a chimney-dependent solar crop dryer. *Solar Energy*, *85*(7), 1560–1573. https://doi.org/10.1016/j.solener.2011.04.019

[9] Afriyie, J. K., & Bart-Plange, A. (2012). Performance Investigation of a Chimney-Dependent Solar Crop Dryer for Different Inlet Areas with a Fixed Outlet Area. *ISRN Renewable Energy*, *2012*, 1–9. https://doi.org/10.5402/2012/194359

[10] Afriyie, J. K., Nazha, M. A. A., Rajakaruna, H. and Forson, F. K. (2013). Mathematical modelling and validation of the drying process in a chimney-dependent Solar Crop Dryer. *Energy Conversion and Management 67, 103-116*.

[11] Daimallah, A., Lebbi, M., and Lounici, M.S., (2022). Effect of The Tower-Chimney Form on The Flow Behaviour Inside a Solar Chimney Power Plant. *Topical Problems of Fluid Mechanics 2022*, Institute of Thermomechanics of the Czech Academy of Sciences, https://doi.org/10.14311/tpfm.2022.005

[12] Bouchair, A., (2022). The effect of the altitude on the performance of a solar chimney, *Energy*, vol. 249, p. 123704, ISSN 0360-5442, Elsevier BV, https://doi.org/10.1016/j.energy.2022.123704

[13] Fallah, S. H., and Valipour, M. S. (2022). Numerical investigation of a small scale sloped solar chimney power plant. *Renewable Energy*, *183*, 1-11., https://doi.org/10.1016/j.renene.2021.10.081

[14] Rahman, M., Mashud, M., & Paul, S. (2021). Economic Analysis of Solar Chimney: Literature Review. *Cold Inflow-Free Solar Chimney*, 217-228, Springer, Singapore. https://doi.org/10.1007/978-981-33-6831-6_10

[15] Rahman, M., Chu, C. M., Kumaresen, S., & Yeoh, S. L. (2021). Introduction of Cold Inflow Free Solar Chimney. In *Cold Inflow-Free Solar Chimney* (pp. 1-11). Springer, Singapore, https://doi.org/10.1007/978-981-33-6831-6_1.

[16] Forsberg, C. H. (2021). Forced convection. *Heat Transfer Principles and Applications*, 211–266. https://doi.org/10.1016/b978-0-12-802296-2.00006-8

[17] Farkas, Z., Országh, E., Engelhardt, T., Csorba, S., Kerekes, K., Zentai, A., Süth, M., Nagy, A., Miklós, G., Molnár, K., Rácz, C., Dövényi-Nagy, T., Ambrus, Á., Győri, Z., Dobos, A. C., Pusztahelyi, T., Pócsi, I., and Jóźwiak, Á. (2022). A Systematic Review of the Efficacy of Interventions to Control Aflatoxins in the Dairy Production Chain—Feed Production and Animal Feeding Interventions. MDPI: *Toxins*, *14*(2), 115. https://doi.org/10.3390/toxins14020115

[18] Abdel-Hadi, A., Schmidt-Heydt, M., Parra, R., Geisen, R., & Magan, N. (2011). A systems approach to model the relationship between aflatoxin gene cluster expression, environmental factors, growth and toxin production by Aspergillus flavus. *Journal of the Royal Society Interface*, *9*(69), 757–767. https://doi.org/10.1098/rsif.2011.0482

[19] Ahsan, S., Bhatti, I.A., Asi, M.R., Bhatti, H.W., Sheikh, M.A., 2010. Occurrence of Aflatoxins in maize grains from central areas of Punjab. Pak. Int. J. Agric. Biol. 12, 571-575.

[20] Wu, F., Groopman, J. D., & Pestka, J. J. (2014). Public Health Impacts of Foodborne Mycotoxins. *Annual Review of Food Science and Technology*, *5*(1), 351–372. https://doi.org/10.1146/annurev-food-030713-092431

[21] Hii, C.L., Jangam, S.V., Ong, S.P. and Mujumdar, A. S. (Ed.). Solar Drying: Fundamentals, Applications and Innovations. Transport Phenomena Group, Singapore, 2012, ISBN 978-981-07-3336-0. p 150.

[22] Schiavone, D. F. (2011). Development and Evaluation of a Natural-Convection Solar Dryer for Mango in Rural Haitian Communities. M.Sc Thesis. University of Florida, USA.

[23] Raju, R. V. S., Reddy, R. M. and Reddy, E. S. (2013). Design and Fabrication of Efficient Solar Dryer. *Journal of Engineering Research and Applications*, *3*(6): 1445–1458.

[24] Seveda, M.S., 2013. Design of a photovoltaic powered forced convection solar dryer in NEH region of India. *International Journal of Renewable Energy Research (IJRER)*, *3*(4), pp.906-912.

[25] Lingayat, A. B., Chandramohan, V. P., Raju, V. R. K., and Meda, V. (2020). A review on indirect type solar dryers for agricultural crops–Dryer setup, its performance, energy storage and important highlights. *Applied Energy*, *258*, 114005. https://doi.org/10.1016/j.apenergy.2019.114005.

[26] El-Sebaii, A. A., and Shalaby, S. M. (2012). Solar drying of agricultural products: A review. Renewable and Sustainable Energy Reviews, 16(1), 37–43. https://doi.org/10.1016/j.rser.2011.07.134

[27] Lingayat, A. B., Chandramohan, V. P., Raju, V. R. K., and Meda, V. (2020). A review on indirect type solar dryers for agricultural crops – Dryer setup, its performance, energy storage and important highlights. Applied Energy, 258, 114005. https://doi.org/10.1016/j.apenergy.2019.114005

[28] Benhamza, A., Boubekri, A., Atia, A., Hadibi, T., and Arıcı, M. (2021). Drying uniformity analysis of an indirect solar dryer based on computational fluid dynamics and image processing. *Sustainable Energy Technologies and Assessments*, *47*, 101466. https://doi.org/10.1016/j.seta.2021.101466

[29] Nasution, I. S., Agustina, R., and Fauza, M. A. (2022). Deep bed drying performance on paddy using hybrid infrared-solar dryer. *IOP Conference Series: Earth and Environmental Science*, *951*(1), 012101. https://doi.org/10.1088/1755-1315/951/1/012101

[30] Abedini, E., Hajebzadeh, H., Mirzai, M. A., Alahdadi, A. A., Ahmadi, H. M., Salehi, M. A., and Zakeri, M. (2022). Evaluation of operational parameters for drying shrimps in a cabinet hybrid dryer. *Solar Energy*, *233*, 221–229. https://doi.org/10.1016/j.solener.2022.01.045

[31] Radhakrishnan Govindan, G., Sattanathan, M., Muthiah, M., Ranjitharamasamy,

S. P., and Athikesavan, M. M. (2022). Performance analysis of a novel thermal energy storage integrated solar dryer for drying of coconuts. *Environmental Science and Pollution Research*. https://doi.org/10.1007/s11356-021-18052-7

[32] Senthil, R., Vijayan, G., Phadtare, G., and Gupta, B. (2021). Performance Enhancements of Solar Dryers Using Integrated Thermal Energy Storage: A Review. *Lecture Notes in Mechanical Engineering*, 355–362. https://doi.org/10.1007/978-981-15-9678-0_31

[33] Treglia, Matt (2015), Understanding Design of Experiments, Quality Digest, Accessed: April 9, 2022; Source: https://www.qualitydigest.com/inside/quality-insider-article/understanding-design-experiments-031215.html

[34] Montgomery, D. C. (2020). *Design and analysis of experiments* (8th ed.). Wiley.